UNIVERSIDAD DISTRITAL
FRANCISCO JOSÉ DE CALDAS

Revista Científica

http://revistas.udistrital.edu.co/ojs/index.php/revcie/index

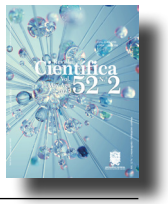

Artículo de investigación científica

Seasonal Analysis of Dissolved Organic Carbon in a Tropical Wetland Using UAV Technology

Análisis estacional del carbono orgánico disuelto en un humedal tropical con tecnología UAV

Análise sazonal do carbono orgânico dissolvido em um pantanal tropical com tecnologia de VANT

Wilfer David Guzman López[1]
Lina Claudia Giraldo[2]
Fabio Velez Macias[3]
Néstor Aguirre[4]

Recibido: 6 de mayo de 2025 **Aceptado:** 25 de septiembre de 2025

Para citar este artículo: Guzman, W. D., Giraldo, L. C., Velez, F. V. y Aguirre, N. (2025). Seasonal Analysis of Dissolved Organic Carbon in a Tropical Wetland Using UAV Technology. *Revista Científica*, *52*(2), 5-20. https://doi.org/10.14483/23448350.23603

Resumen

El carbono orgánico disuelto (COD) desempeña un papel fundamental en el ciclo global del carbono y en la dinámica biogeoquímica de los ecosistemas acuáticos. En este estudio se aplicó un modelo empírico a imágenes de vehículos aéreos no tripulados obtenidas en dos periodos hidrológicos (aguas bajas en febrero y altas en diciembre), en aras de evaluar la dinámica estacional del COD en el humedal El Eneal. La prueba de Kruskal-Wallis reveló diferencias significativas (p=0.00015) en las concentraciones de COD entre ambos periodos, confirmando el efecto regulador del nivel hídrico. Los cambios observados en las firmas espectrales sugirieron variaciones en la composición molecular del COD, con mayor reflectancia azul en aguas altas. Las reducciones de hasta 18 % en zonas vegetadas se atribuyeron a procesos de dilución, retención y mineralización, mientras que las áreas sin vegetación mostraron solo un 2 % de disminución. Estos resultados destacan el papel del ciclo hidrológico en la dinámica de los humedales tropicales.

Palabras clave: carbono orgánico disuelto, limnología, vehículo aéreo no tripulado, humedal tropical, imágenes RGB, análisis espectral, métodos estadísticos no lineales

1. Profesor de cátedra en la Facultad de Ingeniería, Universidad de Antioquia, wilfer.guzman@udea.edu.co
2. Docente en la Facultad de Ingeniería, Universidad de Antioquia, lina.giraldo@udea.edu.co
3. Docente jubilado de la Facultad de Ingeniería, Universidad de Antioquia, fabio.velez@udea.edu.co
4. Docente en la Facultad de Ingeniería, Universidad de Antioquia, nestor.aguirre@udea.edu.co

Abstract
Dissolved organic carbon (DOC) plays a key role in the global carbon cycle and the biogeochemical dynamics of aquatic ecosystems. In this study, an empirical model was applied to imagery from unmanned aerial vehicles, which were acquired during two hydrological periods (low water in February and high water in December), in order to assess the seasonal dynamics of DOC in El Eneal wetland. The Kruskal-Wallis test revealed significant differences (p=0.00015) in the DOC concentrations between periods, confirming the regulatory effect of the water level. Shifts in spectral signatures indicated variations in the molecular composition of DOC, with an increased blue reflectance observed during the high-water period. Reductions of up to 18% in vegetated zones were attributed to dilution, retention, and mineralization processes, whereas unvegetated areas exhibited only a 2% decrease. These findings underscore the influence of the hydrological cycle on DOC dynamics in tropical wetlands.
Keywords: dissolved organic carbon, limnology, unmanned aerial vehicle, tropical wetland, RGB imagery, spectral analysis, multivariate statistical methods

Resumo
O carbono orgânico dissolvido (COD) desempenha um papel fundamental no ciclo global do carbono e na dinâmica biogeoquímica dos ecossistemas aquáticos. Neste estudo, aplicou-se um modelo empírico a imagens obtidas por veículos aéreos ñao tripulados em dois períodos hidrológicos distintos (águas baixas em fevereiro e águas altas em dezembro), visando avaliar a dinâmica sazonal do COD no ecossistema alagado El Eneal. O teste de Kruskal-Wallis revelou diferenças significativas (p=0.00015) nas concentrações de COD entre os dois períodos, confirmando o efeito regulador do nível hidrológico. Alterações nas assinaturas espectrais sugeriram variações na composição molecular do COD, com maior refletância na faixa do azul durante o período de águas altas. Reduções de até 18% em áreas vegetadas foram atribuídas a processos de diluição, retenção e mineralização, enquanto zonas sem cobertura vegetal apresentaram apenas uma diminuição de 2%. Esses resultados destacam o papel central do ciclo hidrológico na dinâmica dos ecossistemas alagados tropicais.
Palavras-chaves: carbono orgânico dissolvido, limnologia, veículo aéreo não tripulado, área úmida tropical, imagens RGB, análise espectral, métodos estatísticos multivariados

INTRODUCTION

Dissolved organic carbon (DOC) is a key component of aquatic ecosystems, and it plays essential roles in the biogeochemical carbon cycle, nutrient bioavailability, and trophic dynamics (Porcal *et al.*, 2009). However, its presence in inland waters leads to water darkening, disrupts the balance between algal photosynthesis and respiration, and can limit primary production by attenuating solar radiation (Thrane *et al.*, 2014; von Einem & Graneli, 2010).

In aquatic systems, DOC primarily originates from the leaching of degraded terrestrial organic matter into freshwater bodies (Pagano *et al.*, 2014). Additionally, it can be generated *in situ* through primary producer activity and the heterotrophic decomposition of plant material (Lønborg *et al.*, 2020).

DOC dynamics in inland waters are influenced by temporal hydrological fluctuations such as precipitation, changes in water level, and temperature variation, as shown in several studies conducted in lentic systems across complete seasonal cycles (Sobek *et al.*, 2007; Pagano *et al.*, 2014; Toming *et al.*, 2020; Zhu *et al.*, 2022; Liu *et al.*, 2023). Despite its sensitivity to environmental changes, *in situ* DOC measurement remains costly and labor-intensive, limiting the spatial and temporal resolution of monitoring efforts.

In recent years, remote sensing technologies using unmanned aerial vehicles (UAVs) have emerged as effective tools for estimating water quality-related optical parameters such as chromophoric dissolved organic matter (CDOM), turbidity, and total suspended solids (TSS). However, their direct application to DOC estimation remains limited. For instance, a global review reported a sharp increase in studies employing UAVs for optical monitoring, albeit highlighting a notable scarcity of research focused specifically on DOC (Pillay *et al.*, 2024). A pioneering study by El Alem *et al.* (2024), however, successfully estimated DOC concentrations in inland waters using UAV-based hyperspectral imagery. They identified six carbon-sensitive spectral bands and achieved R^2 values of 0.86 (using UAV data alone) and 0.92 (when integrating UAVs with satellite observations)—marking a significant advancement in the use of remote sensing for DOC monitoring.

To date, most of these developments have been applied in temperate ecosystems with a well-defined seasonality. In contrast, tropical regions such as El Eneal floodplain lagoon (EEFL) remain poorly characterized in terms of DOC dynamics under complex hydrological regimes. These systems exhibit an atypical seasonality, with bimodal precipitation patterns and pronounced hydrological fluctuations, whose influence on DOC has not been thoroughly investigated (Ríos *et al.*, 2008, 2009). Despite growing access to UAV-based tools and spectral modeling techniques, there remains a substantial gap in their application to tropical seasonal wetlands, particularly those with endorheic conditions and high environmental variability.

These ecosystems play a critical role in carbon storage, hydrological regulation, and biodiversity maintenance, but they face increasing threats arising from climate change and anthropogenic pressures. The pronounced hydrological variability of tropical endorheic wetlands may drive nonlinear responses in DOC concentrations, with important implications for biogeochemical processes and water quality. However, high-resolution, accessible tools capable of capturing these dynamics in detail are still lacking. Thus, UAVs equipped with optical sensors offer a promising opportunity to monitor DOC at fine spatial and temporal scales, providing valuable data to support the management and conservation of these fragile ecosystems. This growing demand for timely, cost-effective environmental information is the primary motivation for this study.

Against this backdrop, we ask: *how does DOC vary seasonally in the EEFL during high- and low-water periods, and which environmental factors modulate these variations?* We hypothesize that seasonal water level fluctuations drive DOC dynamics, with lower concentrations during high-water periods due to dilution processes associated with the endorheic nature of the system.

This study aims to characterize the seasonal variability of DOC in the EEFL using an empirical model applied to UAV imagery captured during contrasting phases of the hydrological cycle (February and December 2024). This methodological approach, which integrates high-resolution remote sensing and advanced spatial analysis, provides essential information to support the long-term preservation and sustainable management of tropical wetlands.

METHODOLOGY

Study area

This study was conducted in the EEFL, a water body located in the municipality of San Onofre, in the department of Sucre, in the Colombian Caribbean region (9°31'30" N, 75°34'48" W). This coastal wetland is part of the wetland complex associated with the Gulf of Morrosquillo and covers approximately 36 ha, with depths ranging from 0.5 to 2.5 m depending on the hydrological regime (Figure 1) (Ríos *et al.*, 2008, 2009).

El Eneal experiences a tropical climate, with a mean annual temperature of 28 °C and an average annual rainfall of 1200 mm, distributed in a bimodal pattern with both rainy seasons (May-June and October-November) and dry seasons (December-April and July-August). The ecosystem is surrounded by vegetation typical of tropical dry forests and mangroves (Castaño, 1999; Mira *et al.*, 2019).

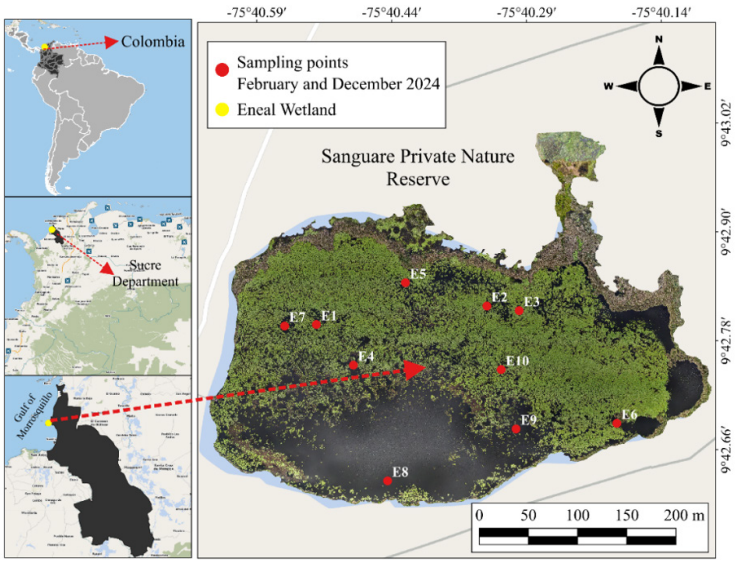

Figure 1. *Study area*

Sample collection and analysis

Two sampling campaigns were conducted during the low-water (29 February 2024) and high-water (5 December 2024) periods. In each campaign, water samples were collected to determine the following parameters: DOC, total dissolved solids (TDS), TSS, turbidity, chlorophyll-*a*, and water transparency. Samples were taken from a depth of 10 cm from ten randomly selected sites via the random point function in ArcGIS Pro. The same sampling sites were maintained across both campaigns in order to ensure results comparability between hydrological periods.

Turbidity was measured *in situ* using a previously calibrated Hach 2100Q turbidimeter, while water transparency was assessed with a 30 cm diameter Secchi disk. Water transparency and TSS were only measured during the sampling campaign conducted on December 5th, 2024 (high-water period). The samples for laboratory analysis were preserved in portable coolers at 0-4 °C and transported to the laboratory within 24 hours of collection.

The laboratory analyses conducted followed standardized protocols: DOC was quantified at the GDCON Laboratory, while TDS and TSS were analyzed at the Environmental Studies Laboratory (LEA). Both laboratories followed the guidelines established in the *Standard methods for the examination of water and wastewater* (APHA, 2017). Chlorophyll-*a* was determined at the Sanitary Hydrobiology Laboratory of Universidad de Antioquia, following the methodology described by Aguirre (2013).

The water levels of the EEFL were measured monthly from February to December 2024, using a limnimeter located at the lagoon's dock. Precipitation and temperature data for the same period were obtained from the DHIME platform (IDEAM), San Onofre station, Sucre, which provides open-access data (Figure 2).

Figure 2. *Limnimeter installed in the EEFL*

Photogrammetric UAV flights

Aerial imagery was acquired through photogrammetric flights using a DJI Phantom 4 Pro V2 UAV, which was equipped with a 1-inch RGB camera and a 20-megapixel CMOS sensor (Figure 3). Flight missions, at an altitude of 120 m, were planned using the Pix4D Capture application, yielding a spatial resolution of 3 cm/pixel. Operations were conducted between 11:00 and 13:00 under clear-sky conditions and wind speeds below 10 $m \cdot s^{-1}$.

The captured images were processed in Agisoft Metashape 10.2 in order to generate orthomosaics, following the methodology described by Cillero Castro *et al.* (2020) and Isgró *et al.* (2022). These orthomosaics were georeferenced in ArcGIS Pro using ground control points. No atmospheric correction was applied since short-range remote sensing involves a negligible atmospheric layer between the sensor and the target surface.

Figure 3. *DJI Phantom 4 Pro V2*

Empirical model

The empirical model used to estimate DOC concentrations from RGB imagery captured during UAV flights was originally developed in the master's thesis by Guzmán (2025). This model defines an exponential relationship between the reflectance values of the red (B1), green (B2), and blue (B3) visible spectral bands and the field-measured DOC concentrations. Specifically, the model uses the ratio of blue to red reflectance (B3/B1) as the independent variable (X) and the estimated DOC concentration as the dependent variable (Y). The mathematical expression of the model is presented below.

$$Y = 14.26e^{-0.1393X} \tag{1}$$

where:

- Y = estimated DOC concentration (mg/L)
- X= ratio of reflectance values from bands B3 (blue) and B1 (red), *i.e.*, $X=B3/B1$

Seasonal analysis

The aquatic vegetation within the wetland was initially masked. To this effect, we evaluated two vegetation indices, *i.e.*, the visible atmospherically resistant index (VARI) and the global leaf index (GLI). We used the following thresholds: VARI > 0.00 and GLI > 0.00. The index yielding the highest classification accuracy was selected to generate a binary mask, which was then subtracted from the original raster to obtain an image representing only the water surface. The mathematical expressions of these indices are shown below:

$$GLI = \frac{\left(2 \times Green - Red - Blue\right)}{\left(2 \times Green + Red + Blue\right)} \tag{2}$$

$$VARI = \frac{\left(Gree - Red\right)}{\left(Green + Red - Blue\right)} \tag{3}$$

Following vegetation masking, pixel-by-pixel subtraction was performed between the DOC distribution rasters for December (high-water period) and February (low-water period). These rasters had been previously generated by applying the exponential empirical model shown in Equation (1) to the water-only masked images. This operation was conducted using the Raster Calculator tool in ArcGIS Pro, enabling the identification of areas where DOC concentrations increased (positive values) or decreased (negative values) between the two periods.

To identify spatial patterns of variation, the K-means clustering algorithm was applied. This unsupervised classification method groups pixels into K clusters based on the similarity and proximity of their spatial characteristics (MacQueen, 1967; Park & Choi, 2022).

Finally, the Kruskal Wallis test, a non-parametric method, was used to statistically validate differences in DOC concentrations relative to the limnimetric levels of the lagoon. This test is suitable when the assumption of normality is not met, and it evaluates differences in group medians by ranking the data (Kruskal & Wallis, 1952; Weaver *et al.*, 2017).

RESULTS

Table 1 presents the laboratory DOC measurements and the radiometric brightness values captured by the sensor in different spectral bands. The DOC concentration ranged from 11.45 to 13.31 mg/L across the two periods, with mean values of 12.77 mg/L in February and 11.80 mg/L in December, indicating a decrease in the latter. Variability was higher in February (standard deviation: 0.29 mg/L) than in December (0.25 mg/L).

The TDS decreased markedly from 696.56 mg/L in February to 250.00 mg/L in December. In December, the mean water transparency, measured with the Secchi disk, was 0.62 m, while the TSS ranged from < 5.00 to 18.00 mg/L. Turbidity also declined between February (6.91 NTU) and December (3.98 NTU).

Moreover, the chlorophyll-*a* concentrations increased from February (mean: 0.54 µg/L; range: 0.15-1.23 µg/L) to December (mean: 1.44 µg/L; range: 0.60-2.38 µg/L). The spectral band values decreased between the two periods: the red band dropped from a mean of 132.00 to 33.10, the green band from 125.50 to 35.20, and the blue band from 111.90 to 42.00, with all bands showing greater variability in February. Regarding the radiometric values captured by the sensor, all spectral bands exhibited a pronounced decrease between periods, particularly in the red and green bands. While all bands displayed relatively symmetric distributions, variability was consistently higher in February.

Table 1. *Laboratory data and spectral bands (February and December 2024)*

Month	Sampling point	DOC (mg/L)	TDS (mg/L)	Secchi (m)	Turb. (NTU)	TSS (mg/L)	Chloroph(µg/L)	B1 (red)	B2 (green)	B3 (blue)
February	E1	12.64	691.9	--	7.79	--	0.74	117	109	97
February	E2	12.93	698.46	--	6.37	--	0.3	126	120	106
February	E3	12.83	700.92	--	6.18	--	0.6	115	108	99
February	E4	12.76	699.28	--	7.67	--	0.6	124	109	93
February	E5	14.31	694.36	--	6.83	--	0.6	114	110	97
February	E6	13.31	699.28	--	6.26	--	1.04	170	176	158
February	E7	12.58	693.54	--	7.64	--	0.3	121	111	97
February	E8	15.15	697.64	--	7.84	--	0.45	152	153	137
February	E9	12.3	700.92	--	6.43	--	0.15	156	153	139
February	E10	12.81	701.75	--	6.94	--	0.6	127	118	106
December	E1	11.5	256	0.66	4.72	<5.00	2.38	26	28	38
December	E2	11.79	250	0.78	3.39	<5.00	1.19	20	22	26
December	E3	11.66	243	0.45	4.62	6	1.21	18	21	28
December	E4	12.19	246	0.56	3.27	<5.00	1.19	45	45	51
December	E5	11.94	257	0.73	3.94	12	1.84	25	26	39
December	E6	12.13	246	0.56	4.79	18	1.25	26	31	32
December	E7	11.6	253	0.62	3.6	5	2.15	29	30	41
December	E8	12	249	0.65	4.35	<5.00	1.19	65	68	70
December	E9	11.83	253	0.5	3.68	7	1.23	51	50	61
December	E10	11.45	266	0.7	3.39	<5.00	1.19	26	31	34

The limnimetric profile of the wetland was plotted monthly from February to December 2024, revealing a pattern consistent with the seasonal variability of precipitation in the study area (Figure 4a). The lowest water level was recorded in April (1.40 m), while the highest occurred in December (3.10 m). This trend reflects the region's bimodal rainfall regime, which includes two wet seasons (May-June and October-December) alternating with two dry seasons (January-April and July-September). Notably, the wetland's water level exhibited a lagged response to regional precipitation: although the highest rainfall occurred in October, the peak water level (3.10 m) was recorded two months later in December (Figure 4b).

Figure 4. *Limnimetric profile from February to December 2024*

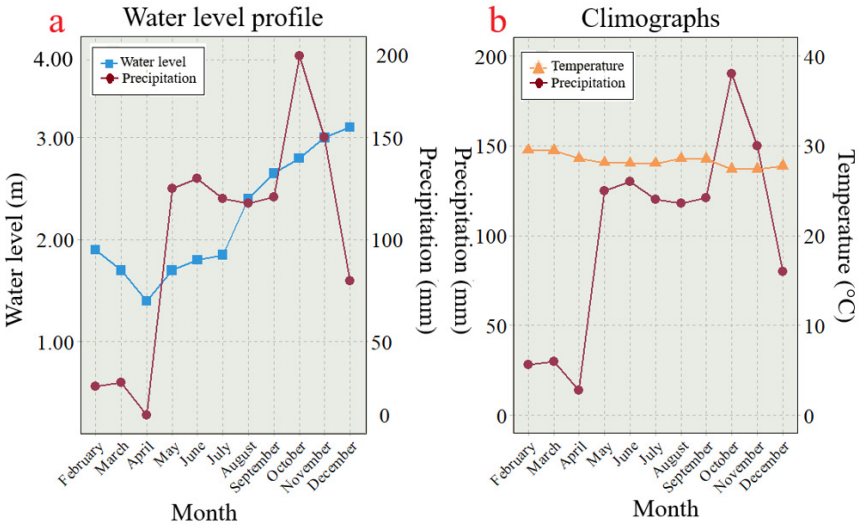

To mask the aquatic vegetation prior to DOC analysis in both periods, the GLI was applied. This index exhibited an effective range between 0.05 and 0.66. In December, greater variability was observed, with values ranging from 0.00 to 0.70. The VARI was also evaluated, but it showed limitations in February due to the predominance of yellowish and brown vegetation.

Subsequently, a subtraction between the February and December 2024 DOC rasters revealed an overall decrease in the DOC concentration during December, as illustrated in Figure 5. The reduction percentages ranged from 0.38 to 18.88%, with a heterogeneous spatial distribution. The southern sector exhibited the smallest decrease, whereas the northern sector, characterized by a higher vegetation cover, showed the largest reduction.

Once the raster of percentage differences in DOC had been obtained, the optimal number of *K* for the K-means algorithm was determined. To this effect, the elbow method, a dendrogram, and R v4.4.2's *NbClust* library (R Core Team, 2018) were employed. The latter includes 26 different criteria for determining the optimal number of clusters. In the elbow method plot, a pronounced change in the decrease of the sum of squared errors (SSE) was observed between $K = 3$ and $K = 4$. The dendrogram analysis revealed a clear hierarchical structure of two groups when the tree was cut at the fifth stage (Figures 6a and 6b). In contrast, the *NbClust* package indicated that ten criteria supported two clusters, six criteria suggested three clusters, and the remaining criteria recommended more than seven clusters (Figure 6c).

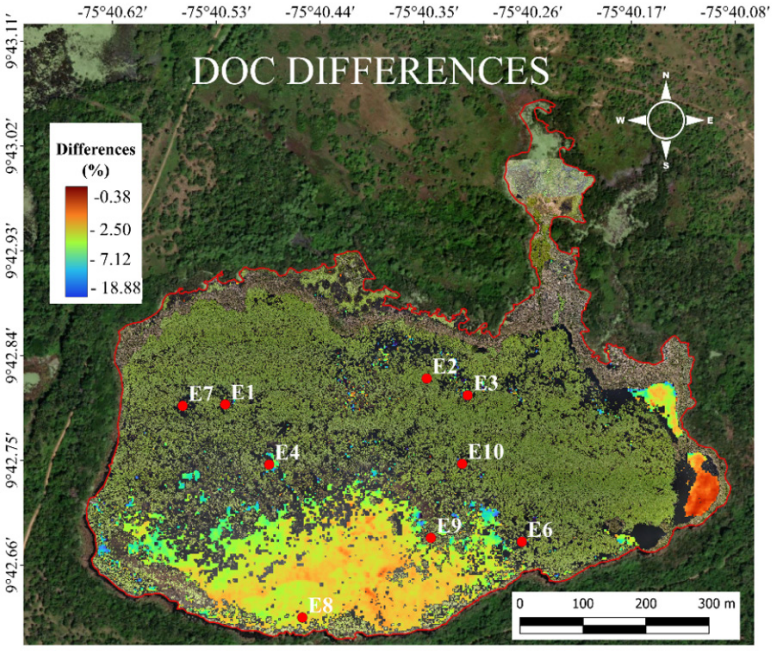

Figure 5. *DOC differences between February and December 2024*

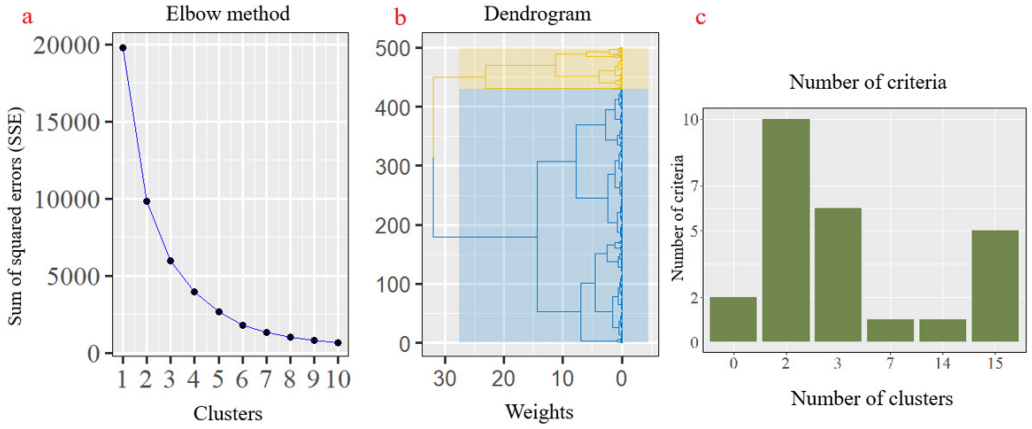

Figure 6. *Cluster number selection criterion*

However, when considering the natural structure of the system, segmentation into two groups appeared to be the most consistent with the characteristics of the area. This system has two clearly distinguishable zones: one with aquatic vegetation and one without. Therefore, the choice of $K = 2$ is consistent with both the system's natural structure and the results of the clustering tests.

Once the optimal K had been selected, the K-means algorithm ($K = 2$) was applied, segmenting the wetland areas according to their percent reduction in DOC. The segmentation results are presented in Figure 7. The yellow region, mainly encompassing the southern part of the lagoon, exhibited a DOC decrease ranging from 0.38 to 5.37%. This zone is characterized by the absence of aquatic vegetation.

Conversely, the blue region reported DOC reductions between 5.37 and 18.88%, concentrated in the northern sector of the wetland. This area is distinguished by a high aquatic vegetation cover and corresponds to the region with the highest recorded DOC reductions (Figure 7).

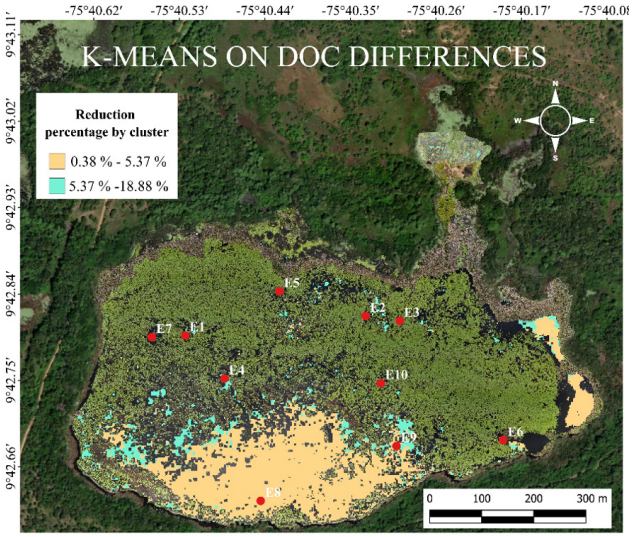

Figure 7. *K-means clustering*

It should be noted that the two zones did not contain the same number of data points, since the water surface was substantially larger in the unvegetated area (yellow region) compared to the vegetated one (blue region). This difference was primarily due to the markedly higher plant biomass observed in December 2024 relative to February 2024. The increased vegetation cover reduced the visible water surface in the vegetated zone, leading to changes in the areas covered by water. Therefore, during pixel-based operations, only values corresponding to intersecting water-covered areas were considered, reflecting a smaller extent of open water in the vegetated regions.

After identifying the seasonal differences in the spatial distribution of DOC via RGB image analysis, these results were statistically validated with *in situ* measurements obtained at different limnimetric levels. Since the data did not meet the assumption of normality, the non-parametric Kruskal-Wallis test was applied, yielding a *p*-value of 0.0001571. This allowed rejecting the null hypothesis of equal medians between DOC concentrations in low- and high-water periods (Figure 8). These results confirm the statistically significant differences between the two periods, highlighting the influence of the limnimetric level on DOC concentrations in the wetland system.

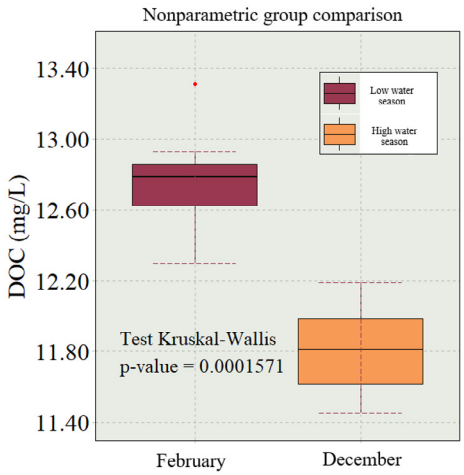

Figure 8. *Nonparametric median test*

DISCUSSION

Effects of increased water levels on the DOC concentration

Our results demonstrate that the water level is a key regulator of DOC concentration in the EEFL, as confirmed by the Kruskal-Wallis test (H=15.32, p=0.00015). This relationship operates mainly through dilution, wherein the increased water volume distributes the same amount of DOC molecules across a larger volume, lowering the concentration (Sobek *et al.*, 2007). In El Eneal, this effect is particularly evident due to the absence of external DOM inputs, which is consistent with the patterns observed in the endorheic lagoons of the Everglades (Harvey & McCormick, 2009). Furthermore, Sobek *et al.* (2007) observed this mechanism across more than 7500 lakes, with major water inputs reducing DOC concentrations by up to 40%, even in the absence of allochthonous sources. In wetlands with higher hydrological connectivity, however, continuous allochthonous DOC inputs may counteract or mask this dilution effect (Cawley *et al.*, 2014; Zhu *et al.*, 2022; Toming *et al.*, 2020). In El Eneal, the absence of such external inputs makes the dilution effect more pronounced. Moreover, increased water levels promote sedimentation by reducing bottom turbulence, which facilitates flocculation and the deposition of organic particles—a particularly relevant process in this shallow system without external turbulence-generating flows (Abbott & Anderson, 2009).

RGB image analysis

The seasonal analysis (February-December) of DOC spatial distribution rasters not only corroborates the statistical findings but also reveals the spatial heterogeneity in concentration reduction. In vegetated areas, the DOC concentration decreased by up to 18.00%, whereas, in unvegetated areas, it was limited to 2.00%. This contrast reflects distinct mechanisms: in vegetated zones, rising water levels in December produced direct dilution and simultaneously favored vegetation expansion (Bornette & Puijalon, 2011; Riis *et al.*, 2012). This expansion increased sediment retention, biofilm development, and microbial activity, enhancing DOC mineralization (Mitsch & Gosselink, 2015). Additionally, the greater water volume reduced sediment resuspension, stabilizing the concentrations. In contrast, in unvegetated zones, the limited 2.00% reduction was largely attributable to dilution alone, with no complementary biological processes. The absence of vegetation increased sediment exposure to wind-driven turbulence, promoting particle resuspension and DOC release (Schulz *et al.*, 2003; Wosnie *et al.*, 2020). The lack of structural barriers also reduced particulate retention, while the scarcity of rhizospheric microbial communities limited biological degradation (Sawant *et al.*, 2023; Zhu *et al.*, 2015). These results reinforce the role of aquatic vegetation as a critical regulator of DOC dynamics by integrating hydrological, physical, and biological processes.

Changes in the optical properties of DOC

Complementing the Kruskal-Wallis results and RGB image analysis, the spectral signature differences between low- and high-water periods suggest variations in DOC optical composition driven by hydrological fluctuations. An inversion pattern was observed: in February, absorption was higher in the blue band, with elevated reflectance in the red band; in December, the reflectance of the blue band increased, while absorption was greater in the red band. These trends align with previous studies documenting DOC optical alterations associated with water volume changes (Anderson *et al.*, 2024; Clark *et al.*, 2020).

To further support these findings, UAV-derived spectral signatures were compared against those of satellite sensors such as Sentinel-2 and Planet. Because of differences in sensor characteristics, all values were normalized prior to comparison. The analysis revealed consistent trends in the spectral responses of DOC under contrasting hydrological conditions (Figure 9). This consistency supports the interpretation that spectral variations reflect changes in DOC composition and concentration, rather than artifacts of sensor technology or spatial scale.

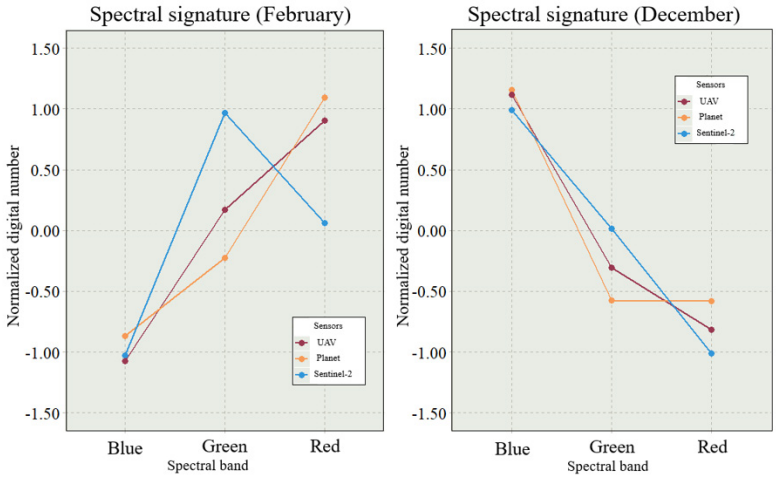

Figure 9. *Water spectral signatures in February and December 2024*

These spectral shifts can be primarily explained by dilution effects during high-water periods, which not only reduce DOC concentrations but also modify optical properties through changes in the molecular composition of humic compounds. The lower DOC concentration observed in December may have favored the dominance of more hydrophilic and less chromophoric fractions, explaining the increased reflectance in the blue band. Similar reductions in absorbance at 254 nm, associated with lower aromaticity and molecular weight, were reported by Tran *et al.* (2022) and Mao *et al.* (2017).

The relevance of these findings is amplified by the low concentrations of chlorophyll-*a*, TSS, and turbidity measured in both sampling periods. These constituents often confound spectral signals by scattering and absorbing light, but the low levels observed minimize their influence. Thus, the observed spectral variations can be more confidently attributed to dissolved organic matter. This reinforces the hypothesis that changes in spectral signatures reflect modifications in DOC composition and concentration rather than interference from other optically active constituents.

Origin of DOC

The endorheic nature of the system, together with the results presented herein, provides strong evidence that DOC in the EEFL is predominantly autochthonous. The main indicator is the direct and predictable response of DOC concentrations to increased water levels (H=15.32, p=0.00015). In systems with significant external inputs, dilution effects are often masked by continuous allochthonous DOC loading, as documented in river-connected or runoff-driven wetlands (Cawley *et al.*, 2014; Liu *et al.*, 2023; Zhu *et al.*, 2022). In El Eneal, the clear manifestation of dilution suggests that DOC concentrations primarily depend on internal production rather than external sources.

Moreover, the high coverage of aquatic vegetation in El Eneal generates substantial plant material that subsequently decomposes into the main DOC source. This process is largely driven by microbial activity, a key factor in autochthonous organic matter production. Studies in comparable endorheic wetlands (Butturini *et al*., 2022; Catalán *et al*., 2013; DeMarty & Prairie, 2009) also reported that, under conditions of abundant aquatic vegetation and limited runoff, DOC is predominantly of autochthonous origin.

CONCLUSIONS

The seasonal analysis of the EELF reveals that rising water levels significantly influence DOC concentration, suggesting a dilution effect during high-water periods. Additionally, changes in the optical properties of water are observed between dry and wet seasons, which is likely linked to molecular variations in DOC composition, such as the proportion of aromatic compounds. A heterogeneous reduction in DOC is also observed: areas with aquatic vegetation exhibit greater decreases, attributable to dilution and mineralization processes, while unvegetated zones maintain higher concentrations, possibly due to particle resuspension and photochemical effects. Nevertheless, these results are preliminary; further sampling campaigns and the inclusion of additional environmental variables are recommended to strengthen these conclusions and improve the understanding of DOC dynamics in the system. Future research should also apply this approach to other tropical wetlands and explore the use of multispectral sensors to refine predictive models.

AUTHOR CONTRIBUTIONS

Wilfer Guzmán López : data curation, investigation, formal analysis, visualization, writing–original draft, review, and editing.
Lina Giraldo Buitrago : funding acquisition, project administration, formal analysis, visualization, writing–original draft, review, and editing.
Fabio Vélez Macías : formal analysis, visualization, writing–original draft, review, and editing.
Néstor Aguirre Restrepo : conceptualization, supervision, project administration, funding acquisition, formal analysis, writing–original draft, review, and editing.

REFERENCES

Abbott, M. B., & Anderson, L. (2009). Lake-level fluctuations. In V. Gornitz (Ed.), *Encyclopedia of Paleoclimatology and Ancient Environments* (pp. 489-492). Springer. https://doi.org/10.1007/978-1-4020-4411-3_121

Aguirre, N. (2013). *Hidrobiología sanitaria*. Facultad de Ingeniería, Universidad de Antioquia.

American Public Health Association (APHA). (2017). *Standard methods for the examination of water and wastewater* (23rd ed.) APHA.

Anderson, K. J., Kominoski, J. S., Osburn, C. L., & Smith, M. A. (2024). Shifting sources and fates of carbon with increasing hydrologic presses and pulses in coastal wetlands. *Journal of Geophysical Research: Biogeosciences, 129*(7), e2023JG007903. https://doi.org/10.1029/2023JG007903

Bornette, G., & Puijalon, S. (2011). Response of aquatic plants to abiotic factors: A review. *Aquatic Sciences, 73*, 1-14. https://doi.org/10.1007/s00027-010-0162-7

Butturini, A., Herzsprung P., Lechtenfeld O. J., Alcorlo P., Benaiges-Fernandez, R. Berlanga, M., Boadella, J., Freixinos Campillo, Z., Gómez, R. M., Sánchez-Montoya, M. M., Urmeneta, J., & Romaní A. M. (2022). Origin, accumulation and fate of dissolved organic matter in an extreme hypersaline shallow lake. *Water Research, 221*, 118727. https://doi.org/10.1016/j.watres.2022.118727

Castaño, L. (1999). *Estudio preliminar de la Ciénaga la Boquilla, municipio de San Onofre* [Undergraduate thesis]. Universidad de Antioquia, Facultad de Ciencias Exactas y Naturales.

Catalán, N., Obrador, B., Felip, M., & Pretus, J. Ll. (2013). Higher reactivity of allochthonous *vs*. autochthonous DOC sources in a shallow lake. *Aquatic Sciences, 75*(4), 581-593. https://doi.org/10.1007/s00027-013-0302-y

Cawley, K. M., Campbell, J., Zwilling, M., & Jaffé, R. (2014). Evaluation of forest disturbance legacy effects on dissolved organic matter characteristics in streams at the Hubbard Brook Experimental Forest, New Hampshire. *Aquatic Sciences, 76*, 611-622. https://doi.org/10.1007/s00027-014-0358-3

Cillero Castro, C., Domínguez Gómez, J. A., Delgado Martín, J., Hinojo Sánchez, B. A., Cereijo Arango, J. L., Cheda Tuya, F. A., & Díaz-Varela, R. (2020). An UAV and satellite multispectral data approach to monitor water quality in small reservoirs. *Remote Sensing, 12*(9), 1514. https://doi.org/10.3390/rs12091514

Clark, C. D., De Bruyn, W. J., Brahm, B., & Aiona, P. (2020). Optical properties of chromophoric dissolved organic matter (CDOM) and dissolved organic carbon (DOC) levels in constructed water treatment wetland systems in southern California, USA. *Chemosphere, 247*, 125906. https://doi.org/10.1016/j.chemosphere.2020.125906

Demarty, M., & Prairie, Y. T. (2009). *In situ* dissolved organic carbon (DOC) release by submerged macrophyte–epiphyte communities in southern Quebec lakes. *Canadian Journal of Fisheries and Aquatic Sciences, 66*(9), 1522-1531. https://doi.org/10.1139/F09-099

El Alem, A., Chokmani, K., Venkatesan, A., Lhissou, R., Martins, S., Campbell, P., Cardille, J., McGeer, J., & Smith, S. (2024). Modeling dissolved organic carbon in inland waters using an unmanned aerial vehicles-borne hyperspectral camera. *Science of The Total Environment, 954*, 176258. https://doi.org/10.1016/j.scitotenv.2024.176258

Guzmán López, W. D. (2025). *Caracterización limnológica del carbono orgánico disuelto en un humedal endorreico tropical mediante detección remota: ciénaga el Eneal, punta norte del golfo Morrosquillo, Colombia* [Master's thesis, Universidad de Antioquia].

Harvey, J. W., & McCormick, P. V. (2009). Groundwater's significance to changing hydrology, water chemistry, and biological communities of a floodplain ecosystem, Everglades, South Florida, USA. *Hydrogeology Journal, 17*(1), 185-201. https://doi.org/10.1007/s10040-008-0379-x

Isgró, M. A., Basallote, M. D., & Barbero, L. (2022). Unmanned aerial system-based multispectral water quality monitoring in the Iberian Pyrite Belt (SW Spain). *Mine Water and the Environment, 41*(1), 30-41. https://doi.org/10.1007/s10230-021-00837-4

Kruskal, W. H., & Wallis, W. A. (1952). Uso de rangos en el análisis de varianza de un criterio. *Revista de la Asociación Americana de Estadística, 47*(260), 583-621.

Liu, F., Zhao, Q., Ding, J., Li, L., Wang, K., Zhou, H., Jiang, M., & Wei, J. (2023). Sources, characteristics, and in situ degradation of dissolved organic matters: A case study of a drinking water reservoir located in a cold-temperate forest. *Environmental Research, 217*, 114857. https://doi.org/10.1016/j.envres.2022.114857

Lønborg, C., Carreira, C., Jickells, T., & Álvarez-Salgado, X. A. (2020). Impacts of global change on ocean dissolved organic carbon (DOC) cycling. *Frontiers in Marine Science, 7*, 466. https://doi.org/10.3389/fmars.2020.00466

MacQueen, J. (1967). *Some methods for classification and analysis of multivariate observations*. https://scispace.com/pdf/some-methods-for-classification-and-analysis-of-multivariate-4pswti19oz.pdf

Mao, R., Li, S. Y., Zhang, X. H., Wang, X. W., & Song, C. C. (2017). Effect of long-term phosphorus addition on the quantity and quality of dissolved organic carbon in a freshwater wetland of Northeast China. *Science of the Total Environment, 586*, 1032-1037. https://doi.org/10.1016/j.scitotenv.2017.02.084

Mira, J. D., Urrego, L. E., & Monsalve, K. (2019). Determinantes naturales y antrópicos de la distribución, estructura y composición florística de los manglares de la Reserva Natural Sanguaré, Colombia. *Revista de Biología Tropical, 67*(4), 810-824. http://dx.doi.org/10.15517/rbt.v67i4.30833

Mitsch, W. J., & Gosselink, J. G. (2015). *Wetlands.* John Wiley & Sons.

Pagano, T., Bida, M., & Kenny, J. (2014). Trends in levels of allochthonous dissolved organic carbon in natural water: A review of potential mechanisms under a changing climate. *Water, 6*(10), 2862-2897. https://doi.org/10.3390/w6102862

Park, J., & Choi, M. (2022). A k-means clustering algorithm to determine representative operational profiles of a ship using AIS data. *Journal of Marine Science and Engineering, 10*(9), 1245. https://doi.org/10.3390/jmse10091245

Pillay, S. J., Bangira, T., Sibanda, M., Kebede Gurmessa, S., Clulow, A., & Mabhaudhi, T. (2024). Assessing drone-based remote sensing for monitoring water temperature, suspended solids and CDOM in inland waters: A global systematic review of challenges and opportunities. *Drones, 8*(12), 733. https://doi.org/10.3390/drones8120733

Porcal, P., Koprivnjak, J. F., Molot, L. A., Dillon, P. J. (2009). Humic substances—Part 7: The biogeochemistry of dissolved organic carbon and its interactions with climate change. *Environmental Science and Pollution Research, 16*, 714-726. https://doi.org/10.1007/s11356-009-0176-7

R Core Team. (2018). *R: A language and environment for statistical computing (version 4.3.3)* [Software]. R Foundation for Statistical Computing. https://www.R-project.org/

Riis, T., Olesen, B., Clayton, J. S., Lambertini, C., Brix, H., & Sorrell, B. K. (2012). Growth and morphology in relation to temperature and light availability during the establishment of three invasive aquatic plant species. *Aquatic Botany, 102*, 56-64. https://doi.org/10.1016/j.aquabot.2012.05.002

Ríos, E. L., Palacio, J. A., & Aguirre, N. J. (2008). Variabilidad fisicoquímica del agua en la ciénaga El Eneal, reserva natural Sanguaré municipio de San Onofre-Sucre, Colombia. *Revista Facultad de Ingeniería Universidad de Antioquia, 46*, 39-45. http://hdl.handle.net/10495/4799

Ríos, E. L., Palacio, J. A., & Aguirre, N. J. (2009). Primary productivity and humic substances in the swamp El Eneal, San Onofre Sucre-Colombia. *Revista Facultad de Ingeniería Universidad de Antioquia, 47*, 67-72. http://hdl.handle.net/10495/5010

Sawant, B., Abeledo-Lameiro, M. J., Gil, Á. G., Couso-Pérez, S., Sharma, S., Sethia, U., & McGuigan, K. G. (2023). Good optical transparency is not an essential requirement for effective solar water disinfection (SODIS) containers. *Journal of Environmental Chemical Engineering, 11*(3), 110314. https://doi.org/10.1016/j.jece.2023.110314

Schulz, M., Kozerski, H. P., Pluntke, T., & Rinke, K. (2003). The influence of macrophytes on sedimentation and nutrient retention in the lower River Spree (Germany). *Water Research, 37*(3), 569-578. https://doi.org/10.1016/S0043-1354(02)00276-2

Sobek, S., Tranvik, L. J., Prairie, Y. T., Kortelainen, P., & Cole, J. J. (2007). Patterns and regulation of dissolved organic carbon: An analysis of 7,500 widely distributed lakes. *Limnology and Oceanography, 52*(3), 1208-1219. https://doi.org/10.4319/lo.2007.52.3.1208

Thrane, J. E., Hessen, D. O., & Andersen, T. (2014). The absorption of light in lakes: Negative impact of dissolved organic carbon on primary productivity. *Ecosystems, 17*, 1040-1052. https://doi.org/10.1007/s10021-014-9776-2

Toming, K., Kotta, J., Uuemaa, E., Sobek, S., Kutser, T., & Tranvik, L. J. (2020). Predicting lake dissolved organic carbon at a global scale. *Scientific Reports, 10*(1), 8471. https://doi.org/10.1038/s41598-020-65010-3

Tran, L. N., Vu, H., & Hall, B. D. (2022). Photosensitizing properties of dissolved organic carbon in Canadian prairie pothole wetland ponds change in response to sunlight. *Canadian Water Resources Journal, 47*(4), 184-201. https://doi.org/10.1080/07011784.2022.2108725

von Einem, J., & Graneli, W. (2010). Effects of fetch and dissolved organic carbon on epilimnion depth and light climate in small forest lakes in southern Sweden. *Limnology and Oceanography, 55*, 920-930. https://doi.org/10.4319/lo.2010.55.2.0920

Weaver, K. F., Morales, V. C., Dunn, S. L., Godde, K., & Weaver, P. F. (2017). *An introduction to statistical analysis in research: With applications in the biological and life sciences*. John Wiley & Sons. https://doi.org/10.1002/9781119454205.ch81

Wosnie, A., Mengistou, S., & Álvarez, M. (2020). Aquatic macrophytes in Ethiopian Rift Valley Lake Koka: Biological management option to reduce sediment loading. *Aquatic Botany, 165*, 103242. https://doi.org/10.1016/j.aquabot.2020.103242

Zhu, M., Zhu, G., Nurminen, L., Wu, T., Deng, J., Zhang, Y., & Ventelä, A. M. (2015). The influence of macrophytes on sediment resuspension and the effect of associated nutrients in a shallow and large lake (Lake Taihu, China). *PLoS One, 10*(6), e0127915. https://doi.org/10.1371/journal.pone.0127915

Zhu, X., Chen, L., Pumpanen, J., Ojala, A., Zobitz, J., Zhou, X., Laudon, H., Palviainen, M., Neitola, K., & Berninger, F. (2022). The role of terrestrial productivity and hydrology in regulating aquatic dissolved organic carbon concentrations in boreal catchments. *Global Change Biology, 28*(8), 2764-2778. https://doi.org/10.1111/gcb.16094